NEW L-BAND SYNTHETIC APERTURE RADAR OBSERVATIONS OF LUNAR SOUTH POLE CRATERS: SEEING INTO COLD TRAPS. G. D. Tolometti[1], S.S.Bhiravarasu[2], G. W. Patterson[3], and C. D. Neish[1]. [1]Department of Earth Sciences/Institute for Earth and Space Exploration, Western University, London, Ontario, N6A 3K7(gtolomet@uwo.ca), [2]Space Applications Centre (ISRO), Ahmedabad, India, [3]Johns Hopkins University Applied Physics Laboratory, Laurel, MD.

Introduction: Radar signals have the ability to penetrate through planetary surfaces and scatter off subsurface interfaces such as lithological layers, buried boulders, or water-ice deposits [1]. It is also capable of "seeing in the dark" in regions where sunlight does not illuminate the surface. New L-band (λ = 24 cm) synthetic aperture radar (SAR) observations acquired by the Indian Space Research Organization's (ISRO) Chandrayaan-2 spacecraft provide additional opportunities for studying the surface and sub-surface properties of polar craters. In particular, we focus on craters containing cold traps within permanently shadowed regions (PSRs) where water-ice deposits are inferred to be present beneath the surface [2,3]. Previous work using Chandrayaan-2 radar data has investigated the radar scattering properties of a select few south polar craters [e.g., 4], in an attempt to find evidence for blocky, near surface deposits of water-ice.

In this work, we have processed over 50 full-polarimetric radar observations acquired by the Chandrayaan-2 spacecraft's dual-frequency SAR (DFSAR) instrument to analyze the surface properties of cold traps mapped by Cannon et al. [3]. To investigate the surface and sub-surface scattering characteristics of cold traps, we calculated the circular polarization ratio (CPR) and degree of linear polarization (DLP). A combination of CPR and DLP provides unprecedented information about both surface and sub-surface features on a planetary body [1], allowing us to infer whether decimetre- to metre-sized (λ = 24 cm) layers are present beneath the lunar regolith. Since radar scattering characteristics are influenced by parameters such as wavelength and incidence angle, we compared our Chandrayaan-2 results to a CPR mosaic generated from monostatic S-band (λ=12.6 cm) radar data acquired by the Lunar Reconnaissance Orbiter (LRO) Miniature-Radio Frequency (Mini-RF) instrument. These data were acquired at shorter wavelengths (S-band) and larger incidence angles (~48°), and thus are sensitive to smaller-scale scattering.

Chandrayaan-2 Observations: We focused our analysis on south polar craters Amundsen, Faustini, Haworth, Malapert, Shoemaker, and Wiechert (Figure 1). All of these craters contain a cold trap identified in Cannon et al. [3] and have been listed as sites of interest for in-situ resource utilization research [e.g., 5]. The DFSAR observations used were acquired at incidence angles of ~26° and slant-range resolutions of 10 × 20 m.

Methodology: We downloaded L-band full-polarimetric Level-1A Slant Range Image (SLI) calibrated data products from the ISRO Science Data Archive. The SLI data are complex image files with each pixel represented by two 4-byte floating values, and each data product containing HH, HV, VH, and VV (H – Horizontal, V – Vertical). Using the polarizations, we generated complex products using the L3Harris Geospatial ENVI program. We then produced covariance matrix products (e.g., C11, C13, C22, and C33) using the publicly available PolSarPro software. We applied a 45 × 1 (Azimuth x Range) multi-look to

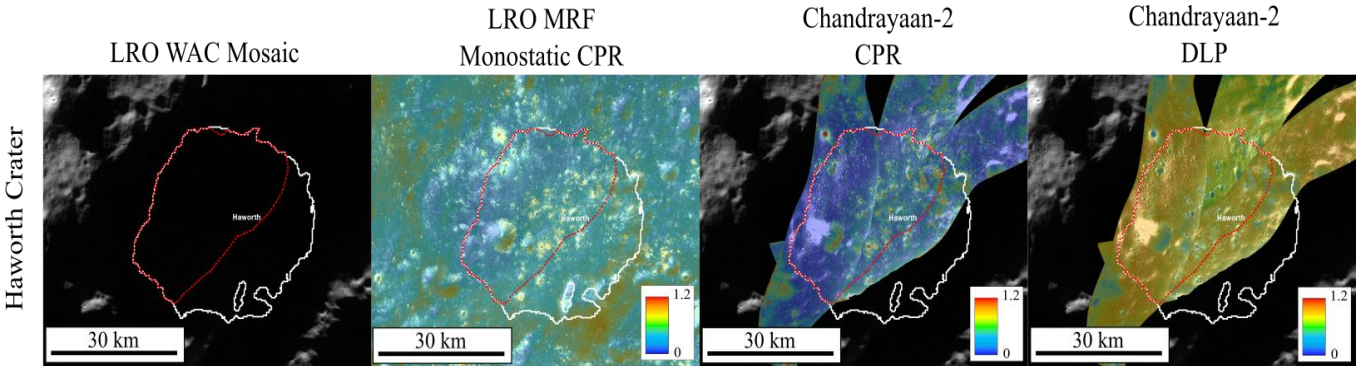

Figure 1. Example of Chandrayaan-2 DFSAR L-band lunar south pole radar data. First column shows a LRO Wide-Angle Camera mosaic of the craters. Figure shows a cold trap inside Haworth crater (Lat -87.4, Long -5.9). Column 2 shows a monostatic CPR mosaic processed from S-band Mini-RF data overlaid on total radar backscatter data. Column 3 shows CPR data calculated from Chandrayaan-2 full-polarimetric L-band radar data overlaid on total radar backscatter data. Column 4 shows DLP data calculated from Chandrayaan-2 full-polarimetric L-band radar data overlaid on total radar backscatter data. Red dashed polygons are data extraction areas, and the white dashed polygons are the margins of cold trap polygons traced by [3].

all of the covariance products to reduce speckle noise and generate square pixels on the SAR output products. Using equations from [6], we calculated the Stokes parameters, which we used to calculate CPR and DLP (Figure 1) [1].

CPR and DLP data were extracted from cold trap regions in the lunar south pole using traced polygons published by [3]. We also extracted data from surfaces outside of the cold traps, to ensure we were observing radar scattering properties that were unique to cold trap environments. We included monostatic CPR data acquired by the LRO Mini-RF instrument in addition to Chandrayaan-2 full-polarimetric data. This allowed us to compare data acquired at different incidence angles, which has a profound effect on radar scattering properties, and at a different wavelength (i.e., S- vs. L-band). Comparing both data sets can provide unique insights regarding the surface and subsurface properties of the lunar south polar region and potentially identify water-ice deposits.

Preliminary Results: Previous work by Bhiravarasu et al., [4] compared the CPR of Mini-RF to full-polarimetric and compact-polarimetric DFSAR data to observe differences in PSR and non-PSR radar scattering properties. Following a similar method, we extracted CPR data from the over 50 full-polarimetric DFSAR L-band observations included in this study and from a Mini-RF monostatic controlled polar mosaic for the craters: Amundsen, Faustini, Haworth, Malapert, Shoemaker, and Wiechert. Mini-RF CPR values from cold traps within those craters are greater than the DFSAR CPR data with a mean of 0.49 vs 0.33 (Figure 2). This difference could be explained by the differences in incidence angles (~26° vs ~47–55°) for the DFSAR and Mini-RF data, respectively, CPR is affected by observation geometry [1]. Alternatively, it is possible that the surface and subsurface features are not as sensitive to L-band (λ = 24 cm) wavelengths, as compared to S-band (λ = 12.6 cm) wavelengths, indicating a smaller scatterer size.

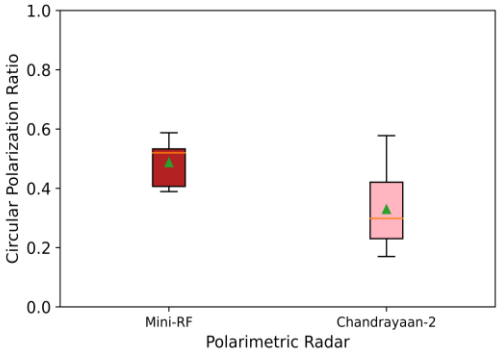

Figure 2. Average CPR data extracted from cold trap regions in the lunar south pole. CPR from LRO Mini-RF monostatic S-band and DFSAR L-band. Data represented as boxplots with green triangle representing the mean, orange lines the median, coloured boxes the interquartile range (50%) and the black lines the maximum and minimum value.

In Figure 3, we observe a general negative trend between the CPR and DLP, with CPR decreasing as DLP increases. Cold traps and surfaces outside of cold traps (i.e. non-Cold Traps in Figure 3) do not show significant differences in CPR or DLP. Craters Haworth and Wiechert show the greatest variation in CPR and DLP values, ranging from moderate CPR (0.58±0.24) to low CPR (0.17±0.1) and high DLP (0.85±0.09) to moderate DLP (0.59±0.13).

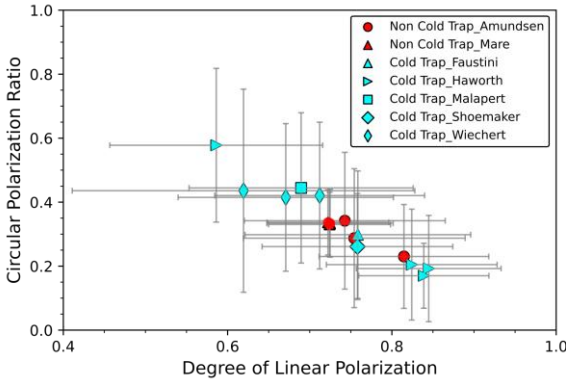

Figure 3. Plot comparing the CPR and DLP values calculated from Chandrayaan-2 full-polarimetric radar data. Cyan points represent cold traps in south polar craters and red points represent surfaces outside of cold traps.

Discussion and Next Steps: From our preliminary results, we observe a negative trend between the CPR and DLP of cold trap surfaces in the lunar south pole. Surfaces returning a low CPR value exhibit a high DLP, which implies the surface and near subsurface is relatively smooth with little to no decimetre- to metre-sized reflectors and that a subsurface layer with different physical properties lies under the overlying regolith (e.g., rock layer). The areas where we extracted moderate CPR and DLP values suggest that decimetre- to metre-sized objects are suspended in the lunar regolith, but not readily exposed on the surface. This is an example of diffuse subsurface scattering and could be attributed to patches of water-ice deposits but could also be linked to large boulders that have been buried in loosely packed regolith. To determine whether this trend is observed in all south polar craters with mapped cold traps, we plan to process new Chandrayaan-2 data products from the next data release cycles in 2022.

References: [1] Carter L. et al. (2011) *Proceedings of IEEE, 99*, 5, 770-782. [2] Spudis P. D. et al. (2013) *JGR: Planets, 118, 10, 2016-2029.* [3] Cannon et al. (2020), *Earth Space Science, 7*, 10. [4] Bhiravarasu et al. (2021) *LPSC LII*, Abstract #1787. [5] Montalvo et al. (2021) *EPSC 2021, 15*. [6] Lee and Pottier (2009) CRC press.